Hindawi
Advances in Materials Science and Engineering
Volume 2023, Article ID 5963742, 8 pages
https://doi.org/10.1155/2023/5963742

Research Article

Characterization of Plastic Deformation in CuZr Metallic Glasses Subjected to the Rolling Process

Ramaswamy Sivaraman,[1] Farag M. A. Altalbawy,[2,3] Alaa Mohammed Hussein Wais,[4] Holya A. Lafta,[5] and Seyedmasoud Hashemi [6]

[1]*Department of Mathematics, Dwaraka Doss Goverdhan Doss Vaishnav College, Arumbakkam, University of Madras, Chennai, India*
[2]*National Institute of Laser Enhanced Sciences (NILES), Cairo University, Giza 12613, Egypt*
[3]*Department of Chemistry, University College of Duba, Tabuk University, Duba 71911, Saudi Arabia*
[4]*Biomedical Engineering Department, Al-Mustaqbal University College, 51001 Hillah, Babil, Iraq*
[5]*Al-Nisour University College, Baghdad, Iraq*
[6]*Department of Chemistry, Iran University of Science and Technology (IUST), Tehran, Iran*

Correspondence should be addressed to Seyedmasoud Hashemi; smhashemi33@gmail.com

Received 3 August 2022; Revised 15 October 2022; Accepted 24 November 2022; Published 21 January 2023

Academic Editor: Shahin Khademinia

Using the rolling process, it is possible to induce multiple shear bands in the microstructure of metallic glasses (MGs) and improve the overall plasticity in the subsequent mechanical loadings. Hence, it is crucial to understand the mechanism of shear banding and plastic deformation under the rolling process. In this work, molecular dynamics (MD) simulation was applied to evaluate the formation and generation of shear bands in a CuZr MG under cold- and hot-rolling processes. Based on the results, it is found that the shear bands are formed with secondary branches in the cold rolling, while the shear events are scattered in the bulk of material in the hot rolling. Considering Voronoi analysis, it is revealed that the hot rolling is accompanied by the recovery of crystalline-like clusters provided that rolling process continues for subsequent passes. On the other hand, the cold-rolled sample shows a stable behavior in the evolution of crystalline-like clusters; however, the population of main icosahedral polyhedrons decreases in the system.

1. Introduction

Metallic glasses (MGs) are in the category of amorphous materials that are known to exhibit superior mechanical properties and excellent functional behaviors [1–4]. However, the poor ductility at room temperature is one of their drawbacks for application in the engineering systems [5–7]. It is generally accepted that the plastic deformation of MGs is occurred in the narrow sheared regions, named as shear bands, which is resulted from the sliding of energetically favorable defects under an external force [8–10]. Recently, many investigations have been conducted to mitigate the brittle behavior of MGs through the formation and interaction of multiple shear bands in the microstructure [11–14]. Although, a single shear band changes to a crack due to the severe strain localization, the multiple shear banding extends plastic deformation in the bulk of specimen [15–18]. Ebner et al. [19] indicated that the high pressure torsion (HPT) induced the extra shear strains in the amorphous structure, leading to improvement of plastic defamation. Boltynjuk et al. [20] reported that the HPT process intensified the structural heterogeneity and increased population of shear bands. In this state, the hardness and elastic modulus declined; however, the strain-rate sensitivity was enhanced in the MG. Astanin et al. [21, 22] revealed that the HPT process increased the shear band

density to more than 1.76 μm^{-1}, while the distance between shear bands were in the range of 80–120 μm. Li et al. [23] demonstrated that the introduction of prestrain and shear bands by one-directional cold rolling led to the significant improvement of fracture toughness in the ZrTiCuNiAl BMG. Moreover, the orientation of preshear bands played a major role in the final mechanical properties. Using molecular dynamics (MD) simulation, Zhao et al. [24] evaluated the influence of prestress on the plasticity and mechanical properties of CuZr MGs under the indenting process. Their results indicated that the morphologies of shear band were affected by the magnitude of prestress so that the catastrophic propagation of shear bands in the nanoindentation process was correlated to the large prestress values. Fan et al. [25] indicated that the 10% prestraining of ZrCuAl amorphous alloy increased the Helmholtz activation energy and generated the population of shear transformation zones (STZs), leading to homogenous plasticity under the subsequent external loading. Another investigation showed that the precold rolling decreased the population and magnitude of pop-ins in the load-displacement curves of nanoindentation test, resulting in a gradual transition from inhomogeneous to homogenous flow behavior [26]. Xie and Kruzic [27] reported that the precold rolling improved the fracture toughness more than 50%, which is due to the promotion of numerous shear bands along the main crack path in the rolled sample. Reddy et al. [13] reported that the hot rolling process induced the scattered thick shear bands in the sample, while the dense fine shear events were distributed in the microstructure under the cryo-rolling process. Scudino et al. [28] investigated the role cold rolling on the mechanical behavior of ZrTiCuNiAl BMG and found that the small plastic strain applied by the pretreatment was efficient for enhancing the plastic deformation under the compressive or tensile loadings. It is a proven idea that the prerolling process is an efficient method for improving the plastic deformation in the MGs. However, the identification of shear-banding in the rolled samples has been a hot topic for tuning the plastic deformation and ultimate strength. In this paper, we aimed to characterize the evolution of shear bands in the rolled MGs and show that how the parameters of rolling process (cold or hot) change the shear-banding features.

2. Modeling and Simulation

2.1. Sample Preparation. The simulation box of $Cu_{54}Zr_{46}$ composition with the dimensions of $30 \times 18 \times 12\ nm^3$ was firstly modeled by the Large-scale Atomic/Molecular Massively Parallel Simulator (LAMMPS) and with the consideration of atomic interactions described through the embedded atom method (EAM) potential [29]. For this purpose, the atomic box was heated to 2000 K and held in a molten state for 2 ns, and then it was cooled down to 300 K with the cooling rate of 10^{11} K/s. It should be noted that the sample preparation was conducted under the NPT ensemble and periodic boundary conditions and time step of 1 fs. It is worth to note that it is possible to simulate a wide range of CuZr composition and prepare various MGs through the MD method. However, we selected the $Cu_{54}Zr_{46}$ composition with the moderate mechanical properties in the CuZr system [30–32].

2.2. Nano-Rolling Process. In the nano-rolling process, two sets of rigid rotating rollers were prepared to reduce the sample thickness for 8% and 12%, respectively (See Figure 1). The lower and upper rollers for both of sets rotated (0.003 rot.·ps^{-1}) in the clockwise and anticlockwise directions, respectively. The first step to model the rolling process is to create the rollers with cylindrical geometry with specified dimensions [13]. The rollers were considered as rigid bodies, meaning that they became quite immune to any plastic deformation in the rolling process. The details of rollers including the dimensions are given in Figure 1. After the creation of rollers, the MG sample moved to the rolling system with a constant velocity of 0.1 nm/ps. The x, y, and z directions in the rolling system were considered as rolling direction (RD), transverse direction (TD), and normal direction (ND), respectively. The shrink-wrapped boundary condition was considered along the transverse direction. Prior to the rolling process, the whole system was relaxed by conjugate gradient technique [33]. The temperatures for the process were kept at 300 K and 650 K, providing conditions for evaluation of cold rolling and hot rolling in the MGs. To achieve a stable system, the temperature was equilibrated under microcanonical ensemble [13]. The Nosé–Hoover thermostat was used to maintain the temperature at the certain values [34]. OVITO package was also employed to visualize the evolution of system under the rolling process [35].

3. Results and Discussion

Figure 2(a) represents the snapshots of shear strain at the normal direction (ND) during the cold rolling (300 K). Moreover, the distribution of shear strain for selected regions are plotted in Figure 2(b). Considering the first stage of rolling process, the plastic deformation is accompanied with the low density and weak generation of shear bands in the microstructure, which is owing to the small percentage of thickness reduction (8%). The strain map also shows that the orientation of shear bands is mainly in the range of 43°–47°. Passing through the second stage of rolling process, the density of shear bands enhances in the system, leading to the high intensification of strained regions. It is suggested that the accumulation of previously-formed shear bands along with the formation of new ones are the main sources of the plastic deformation during the second stage [13]. The mechanism of shear band formation and propagation in our study is similar to that reported in other works focusing on the experimental procedures [36, 37]. Figure 2(b) shows the variations of shear strain in the selected regions. The lines A and C belong to the sides of sample, while the line B introduces the evolution of strain at the middle section of sample. Considering the first stage of rolling process, one can see that the curves of A and C exhibit a uniform trend, in which the strain is maximum at the bottom and top regions,

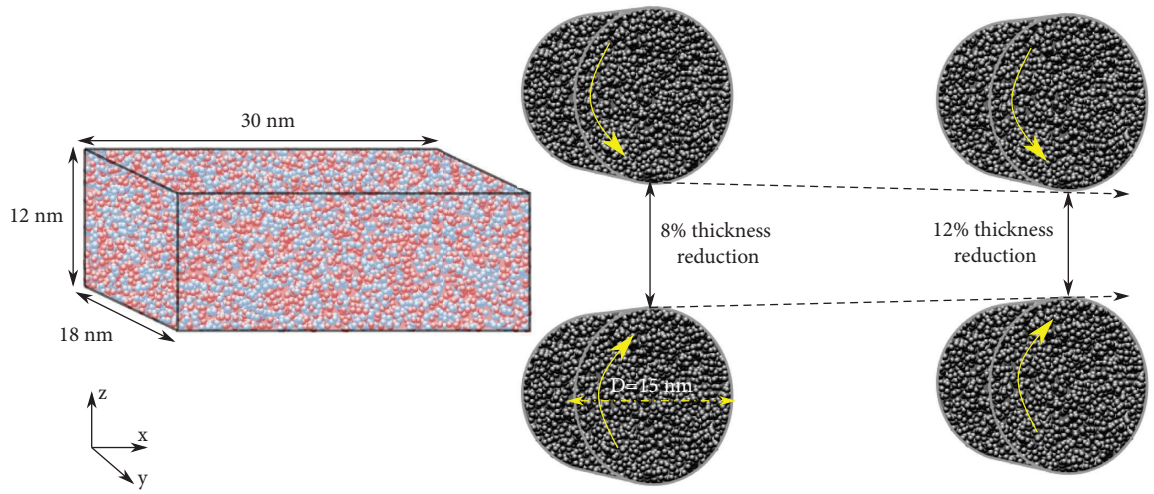

Figure 1: Schematic of rolling process for CuZr MG plate.

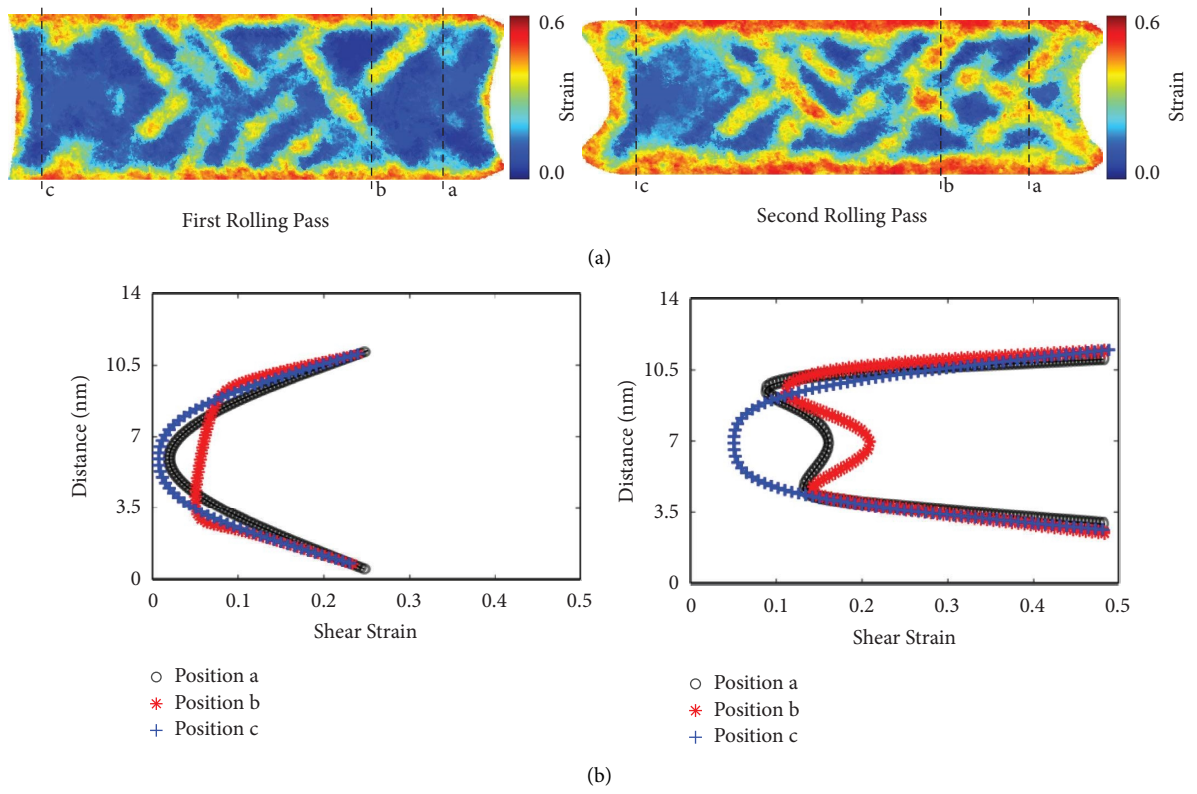

Figure 2: (a) The snapshots of shear strain at the normal direction (ND) during the cold rolling, (b) the linear distribution of shear strain for selected regions.

while the center part includes the minimum strain. The line *B* exhibits a different strain curve with a hump at the center of sample. This event implies that the main shear banding occurs at the center of sample in the position *B*; however, the sheared strain at the sides of sample; i.e. positions *A* and *C*, is mainly restricted near the surfaces. It is suggested that the atoms are constrained at the middle part of sample leading to the strain accumulation at the normal direction and shear band propagation at the center part. On the other hands, the atoms at the sides of the sample can establish cooperative movements at the rolling direction and created strain regions near the surface of sample. Passing through the second stage of rolling process, a higher strain values are accumulated in the bulk of sample, leading to the creation of strain humps in the curves *A* and *B*. This result indicates that the center part of sample is accumulated with the extreme sheared regions, compared with the first stage of rolling process. Moreover, it is observed that all of the strain curves shift to the right side, indicating the total increment of plastic deformation after the second stage of rolling process.

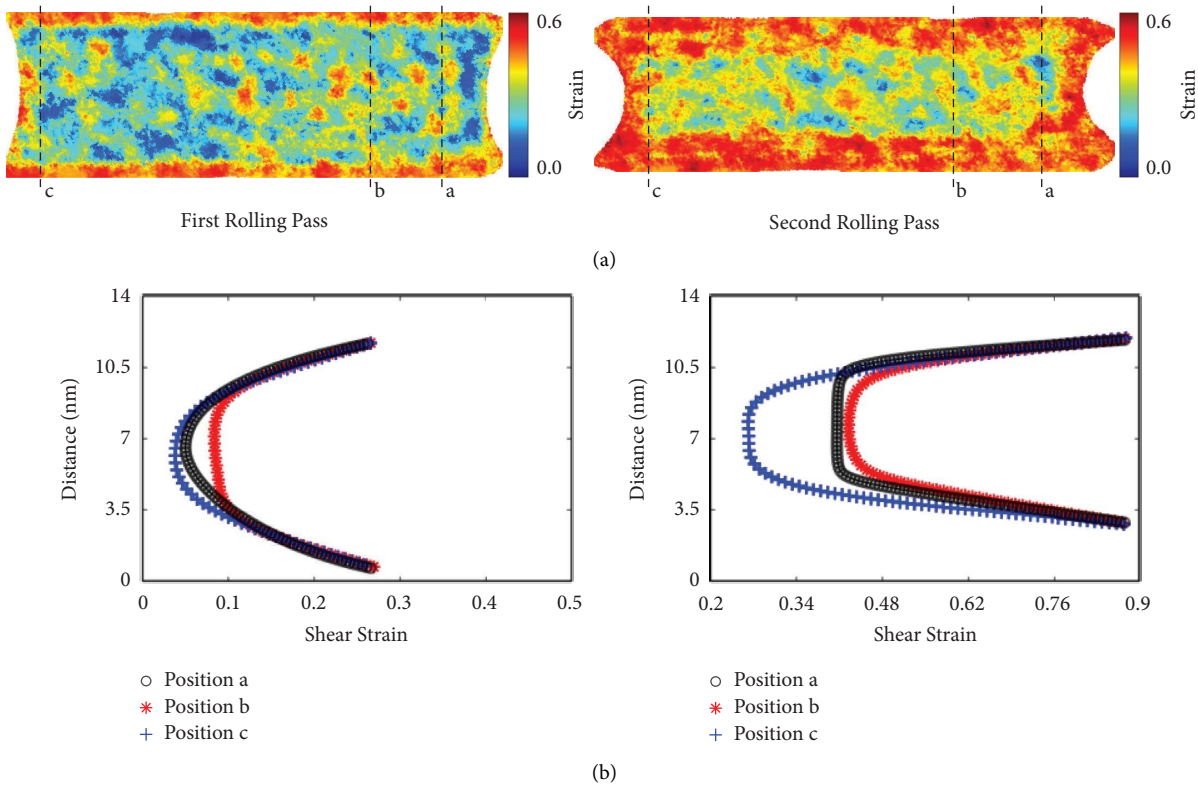

Figure 3: (a) The snapshots of shear strain at the normal direction (ND) during the hot rolling, (b) the linear distribution of shear strain for selected regions.

Figure 3(a) indicates the shear strain snapshots of MG sample rolled in two stages at 650 K. Figure 3(b) shows the variations of shear strain in the selected regions. Compared to the cold rolling, the shear strain was randomly distributed in the microstructure. It is apparent that the density of shear bands is lower in the hot rolling, meaning that the elevated temperature led to the high thermal activity of atoms in the system. Moreover, after the second rolling stage, one can see that the density of shear bands is still low. The trend of strain in the selected regions also shows that there is no sign of serious hump in the curves for both stages of rolling process, implying that the shear banding is not prevailing in the center of specimen at high temperatures. This phenomenon was also detected in other works [13, 38]. Nevertheless, one should note that the shift of curves to the right side at the second stage is much more than the cold rolling process. This means that plastic deformation in the hot rolling process is more homogenous and the nanoscale shear events are randomly distributed in the structure.

In the following, the structural evolution in the cold- and hot-rolled samples is compared and the details of shear-banding mechanism are presented. Figure 4(a) illustrates the atomic strain tensor along the rolling direction for the regions involved with the shear process. According to the results, the cold rolling is accompanied with the formation of primary shear bands with a few second branching evolution. On the other side, the shear transformation zones are homogeneously dispersed in the hot-rolled sample, indicating the uniform plastic deformation, compared to the cold rolling condition. To make a detailed comparison, we evaluated the rotation of the atomic displacement vector, affecting the mechanism of shear banding in the system. Recently, it has been reported that the type of movement and rotation of atoms in the vicinity of shear bands are different from the nonstrained zones [39]. Figure 4(b) represents the scatter data correlating the displacement vector rotations to the atomic shear strain of regions involved in the shear banding. One can see that the rotation angles in the hot rolling is more sporadic in comparison with the cold rolling. Moreover, there are more atomic rearrangements with higher shear strain and rotation angles in deformed part of the hot-rolled sample. This result is consistent with this fact that the higher thermal activity at the elevated temperature enhances the atomic movements, leading to the intensification of displacement vector rotation in a certain shear strain. Figure 4(c) shows the polynomial fitting of the data along with the regression values for cold and hot rolling processes. This information provides conditions for evaluation of the variability from the average value. According to the results, the hot rolling exhibits a lower regression value, demonstrating that the generation of nanoscale strain at elevated temperature is accompanied with the higher displacement and rotation of atoms in the system.

The application of loading in the rolling process induces the plastic deformation and changes the atomic rearrangement in the microstructure [14, 37, 40]. In this investigation, the Voronoi analysis was carried out to find out how the rolling process alters the population of atomic

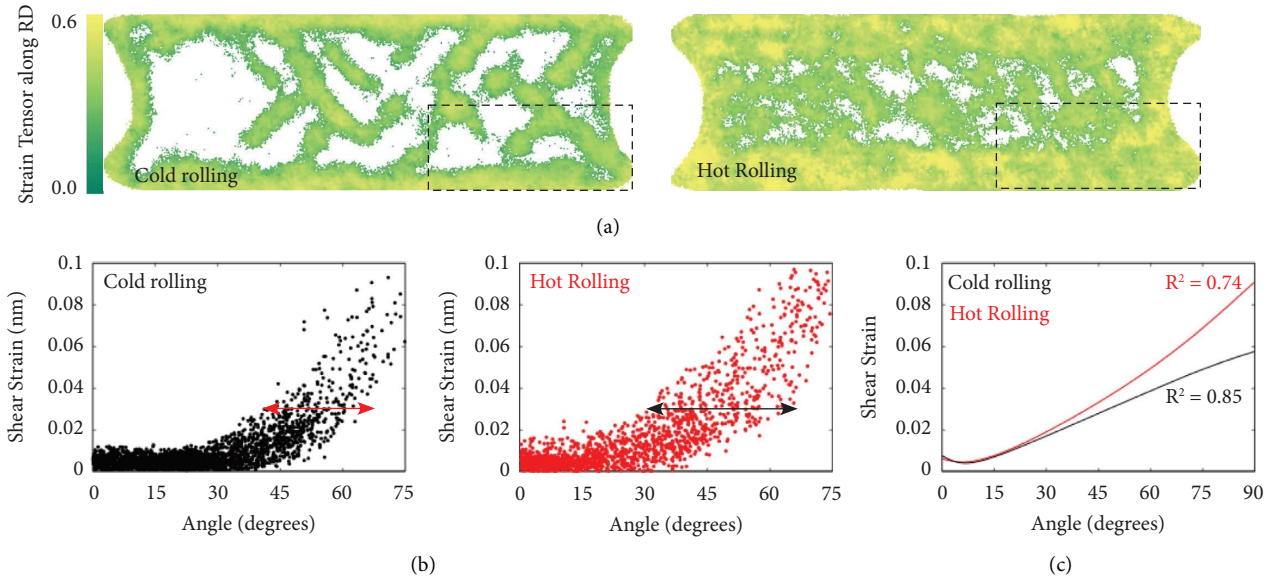

FIGURE 4: (a) Strain tensor snapshots of the rolled samples under cold-and hot rolling conditions, (b) shear strain as a function of displacement angle, (c) polynomial fitting of the plots given in part b.

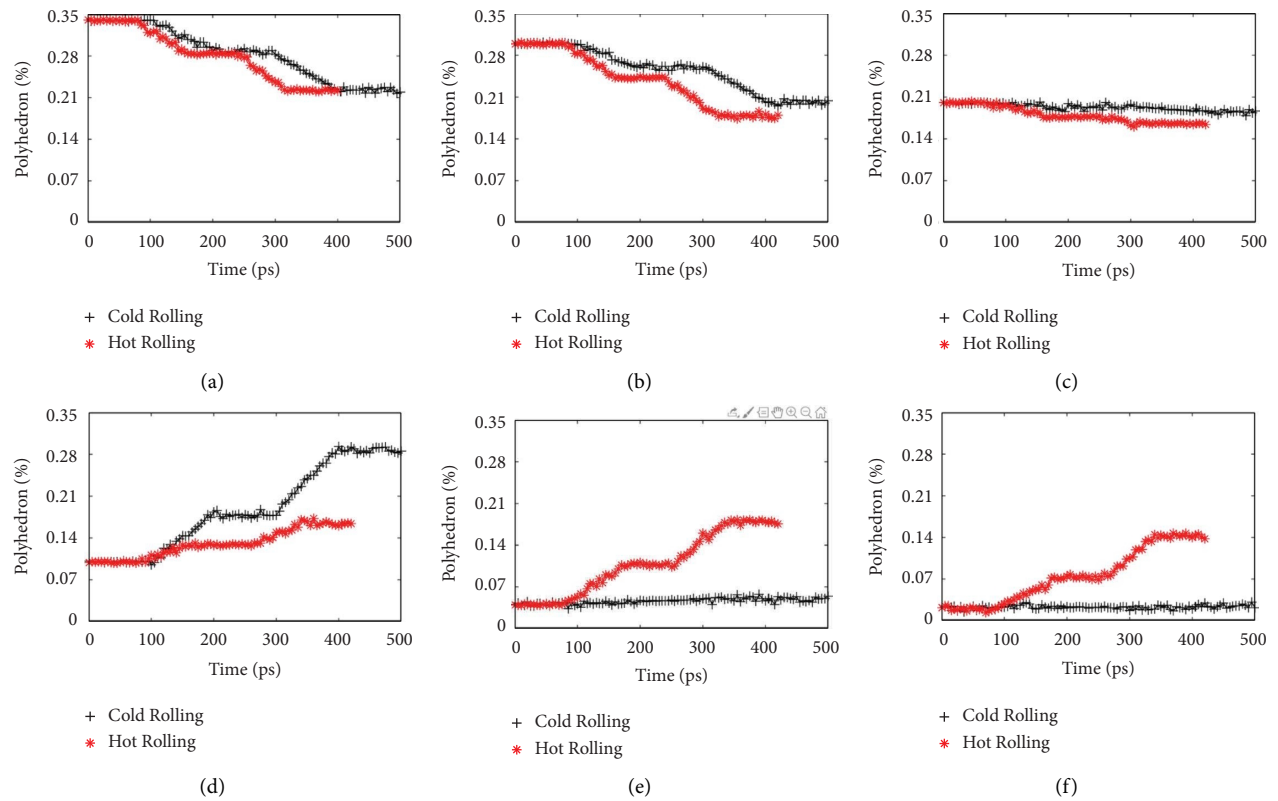

FIGURE 5: Fraction of main polyhedrons as a function of rolling time for (a) <0 0 12 0> (b) <0 2 8 1> (c) <0 1 10 2>, (d) <0 3 6 3 >, (e) <0 4 4 5> and (f) <0 4 4 6>.

clusters [41, 42]. Figure 5 gives the normalized fraction of main coordination polyhedrons under the overall time of nano-rolling at 300 K and 650 K. Firstly, it is observed that there is a plateau part in the plots for all of the conditions. This plateau is associated to the time between the first and second stages of rolling process, in which no compressive load is applied to the sample. As a result, the change in the polyhedron fraction remains constant. Secondly, one should note that many works have shown that the CuZr MGs include numerous types of polyhedrons [43, 44]. In this work,

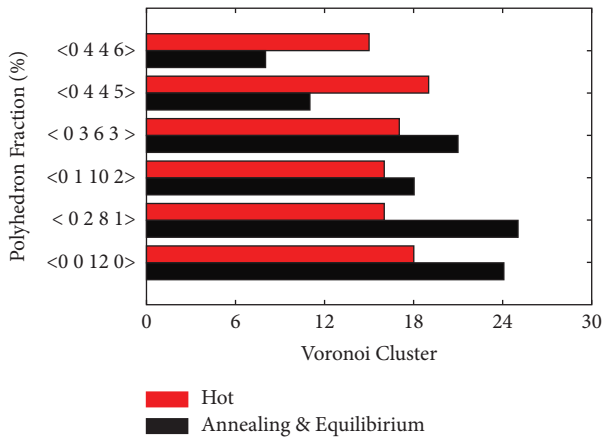

Figure 6: The percentage of main voronoi clusters in the hot rolled and annealed samples.

we selected the main ones comprising the most fraction of clusters as the icosahedral-like clusters and crystal-like clusters in the system. Based on the results, the backbone structure of CuZr sample is dominated by the icosahedral-like clusters with the indices of <0 0 12 0>, <0 2 8 1>, and <0 1 10 2>. Under the rolling process, the polyhedral fractions are markedly changed in the system. In the cold rolling process, a significant decrease occurs in the fraction of <0 0 12 0 > and <0 2 8 1> polyhedrons, while the polyhedron <0 3 6 3 > is mainly recovered. Moreover, polyhedrons <0 1 10 2>, <0 4 4 5>, and <0 4 4 6> show a stable trend during the cold rolling. On the other hand, the crystalline-like polyhedrons, i.e. <0 4 4 5> and <0 4 4 6>, show an increasing trend during the hot rolling process. This outcome indicates that the CuZr MG tends to lose its amorphous nature so that with the rise of thickness reduction, the crystallization may occur in the system [13]. To be sure about our idea, we treated the raw MG sample at 650 K for 1 ns and evaluated the variations of Voronoi polyhedrons after the equilibration. As can be seen in Figure 6, the hot rolling process has more effective in the disintegration of cluster types in the atomic configuration. Moreover, the fractions of polyhedrons <0 4 4 5> and <0 4 4 6> in the relaxed sample are considerably less than the hot-rolled condition. This analysis validates that the application of loading at high temperature influences the amorphous nature of MG sample through the insertion of extra energy into the system, providing energy barrier for crystallization in the microstructure.

4. Conclusion

The cold and hot rolling processes have been carried out to characterize the mechanism of shear banding and plastic deformation in the CuZr MG samples. In accordance with the outcomes of MD simulation, the following conclusions are drawn as follows:

(a) For both of cold and hot states, the density and population of shear bands were limited in the first pass of rolling process, which was due to the lower percentage of thickness reduction. In the second pass, the plastic deformation was extended in the material, which was due to the formation of new shear bands and growth of previous ones.

(b) The local evaluation of strain distribution showed that the cold rolling process was accompanied with the generation of shear bands through the center of sample, while a homogenous shear-strain distribution was observed in the normal direction for the hot-rolled sample.

(c) Considering Voronoi analysis, it is revealed that the hot rolling led to the recovery of crystalline-like clusters, meaning that the glassy structure tends to form crystalline phases. On the other hand, the cold-rolled sample showed a decrease in the population of main icosahedral polyhedrons, while the evolution of crystalline-like clusters remained stable.

Data Availability

All data is available in the manuscript.

Conflicts of Interest

The authors declare that there are no conflicts of interest.

References

[1] Y. Zhang, J. Li, Q. Zhang, S. Ding, W. Wu, and R. Xia, "Tetrachiral nanostructured metallic glasses with mechanically tunable performance," *Materials Chemistry and Physics*, vol. 276, Article ID 125315, 2022.

[2] X. Zhang, L. Lai, S. Xiao et al., "Effect of W on the thermal stability, mechanical properties and corrosion resistance of Fe-based bulk metallic glass," *Intermetallics*, vol. 143, Article ID 107485, 2022.

[3] J. Wegner, M. Frey, M. Piechotta et al., "Influence of powder characteristics on the structural and the mechanical properties of additively manufactured Zr-based bulk metallic glass," *Materials & Design*, vol. 209, Article ID 109976, 2021.

[4] R. Sivaraman, I. Patra, Z. M. Najm, N. M. Hameed, T. Alawsi, and S. Hashemi, "The effects of minor element addition on the structural heterogeneity and mechanical properties of ZrCuAl bulk metallic glasses," *Advances in Materials Science and Engineering*, vol. 2022, pp. 1–8, 2022.

[5] Y. Lu, S. Su, S. Zhang et al., "Controllable additive manufacturing of gradient bulk metallic glass composite with high strength and tensile ductility," *Acta Materialia*, vol. 206, Article ID 116632, 2021.

[6] R. M. O. Mota, E. T. Lund, S. Sohn et al., "Enhancing ductility in bulk metallic glasses by straining during cooling," *Commun. Mater.*vol. 2, pp. 23–28, 2021.

[7] H. Wang, W. Dmowski, Y. Tong et al., "Nonaffine strains control ductility of metallic glasses," *Physical Review Letters*, vol. 128, no. 15, Article ID 155501, 2022.

[8] X. Mu, M. R. Chellali, E. Boltynjuk et al., "Unveiling the local atomic arrangements in the shear band regions of metallic glass," *Advanced Materials*, vol. 33, no. 12, Article ID 2007267, 2021.

[9] X. Li, R. Qu, W. Rao, and X. Jiang, "A new idea of modeling shear band in metallic glass based on the concept of distributed dislocation," *Journal of Non-crystalline Solids*, vol. 577, Article ID 121328, 2022.

[10] I. Patra, A. M. Abdulhadi, F. S. Fahim, B. S. Bashar, T. Alawsi, and M. Salmani, "The effects of temperature and impact velocity on the shock wave response of pore-embedded metallic glasses," *Advances in Materials Science and Engineering*, vol. 2022, pp. 1–8, 2022.

[11] A. Jain, Y. Prabhu, D. Gunderov, E. Ubyivovk, and J. Bhatt, "Study of micro indentation assisted deformation on HPT processed Zr62Cu22Al10Fe5Dy1 bulk metallic glass," *Journal of Non-crystalline Solids*, vol. 566, Article ID 120877, 2021.

[12] K. Nomoto, B. Li, C. Gammer et al., "Deformation-induced medium-range order changes in bulk metallic glasses," *Physical Review Materials*, vol. 6, no. 4, Article ID 043603, 2022.

[13] K. V. Reddy and S. Pal, "Recreating the shear band evolution in nanoscale metallic glass by mimicking the atomistic rolling deformation: a molecular dynamics study," *Journal of Molecular Modeling*, vol. 27, pp. 220–228, 2021.

[14] S. Scudino, "Mechanism of shear banding during cold rolling of a bulk metallic glass," *Journal of Alloys and Compounds*, vol. 773, pp. 883–889, 2019.

[15] X. Lu, S. Feng, L. Li et al., "Severe deformation-induced microstructural heterogeneities in Cu64Zr36 metallic glass," *Modelling and Simulation in Materials Science and Engineering*, 2022.

[16] V. S. Zolotorevsky, A. I. Bazlov, A. G. Igrevskaya, A. S. Aronin, G. E. Abrosimova, and D. V. Louzguine-Luzgin, "Significant mechanical softening of an Al-Y-Ni-Co metallic glass on cold and hot rolling," *Journal of Occupational Medicine*, vol. 71, no. 11, pp. 4079–4085, 2019.

[17] A. Gunti, P. P. Jana, M.-H. Lee, and J. Das, "Effect of Cold Rolling on the Evolution of Shear Bands and Nanoindentation Hardness in Zr41.2Ti13.8Cu12.5Ni10Be22.5 Bulk Metallic Glass," *Nanomaterials*, vol. 11, 2021.

[18] K. E. Avila, S. Küchemann, and H. M. Urbassek, "Interaction between parallel shear bands in a metallic glass," *Journal of Non-crystalline Solids*, vol. 566, Article ID 120882, 2021.

[19] C. Ebner, B. Escher, C. Gammer, J. Eckert, S. Pauly, and C. Rentenberger, "Structural and mechanical characterization of heterogeneities in a CuZr-based bulk metallic glass processed by high pressure torsion," *Acta Materialia*, vol. 160, pp. 147–157, 2018.

[20] E. Boltynjuk, D. Gunderov, E. Ubyivovk et al., "Enhanced strain rate sensitivity of Zr-based bulk metallic glasses subjected to high pressure torsion," *Journal of Alloys and Compounds*, vol. 747, pp. 595–602, 2018.

[21] V. Astanin, D. Gunderov, Z. Q. Ren, R. Valiev, and J. T. Wang, "High density of shear bands in the Vitreloy bulk metallic glass subjected to high-pressure torsion," *IOP Conference Series Materials Science and Engineering*, vol. 1008, no. 1, Article ID 012031, 2020.

[22] D. V Gunderov, V. V Astanin, A. V Sharafutdinov, and J. Bhatt, "Slippage during high-pressure torsion processing of Vitreloy 105 bulk metallic glass," *Journal of Physics: Conference Series*, vol. 1967, Article ID 12062, 2021.

[23] B. Li, S. Scudino, B. Gludovatz, and J. J. Kruzic, "Role of pre-existing shear band morphology in controlling the fracture behavior of a Zr–Ti–Cu–Ni–Al bulk metallic glass," *Materials Science and Engineering A*, vol. 786, p. 139396, Article ID 139396, 2020.

[24] D. Zhao, B. Zhu, S. Wang, Y. Niu, L. Xu, and H. Zhao, "Effects of pre-strain on the nanoindentation behaviors of metallic glass studied by molecular dynamics simulations," *Computational Materials Science*, vol. 186, Article ID 110073, 2021.

[25] H. Fan, N. Wang, C. He, Y. Huang, Z. Ning, and J. Sun, "Effect of pre-straining on the structure and nano-mechanical properties of a CuZrAl bulk metallic glass," *Journal of Alloys and Compounds*, vol. 918, Article ID 165635, 2022.

[26] A. Gunti and J. Das, "Effect of cold rolling on the serrated flow behavior of Zr41.2Ti13.8Cu12.5Ni10Be22.5 bulk metallic glass during nanoindentation," *Journal of Materials Research*, vol. 37, no. 4, pp. 976–989, 2022.

[27] S. Xie and J. J. Kruzic, "Cold rolling improves the fracture toughness of a Zr-based bulk metallic glass," *Journal of Alloys and Compounds*, vol. 694, pp. 1109–1120, 2017.

[28] S. Scudino, B. Jerliu, K. B. Surreddi, U. Kühn, and J. Eckert, "Effect of cold rolling on compressive and tensile mechanical properties of Zr52.5Ti5Cu18Ni14.5Al10 bulk metallic glass," *Journal of Alloys and Compounds*, vol. 509, pp. 128–130, 2011.

[29] M. I. Mendelev, M. J. Kramer, R. T. Ott, D. J. Sordelet, D. Yagodin, and P. Popel, "Development of suitable interatomic potentials for simulation of liquid and amorphous Cu–Zr alloys," *Philosophical Magazine*, vol. 89, no. 11, pp. 967–987, 2009.

[30] C. Tang and C. H. Wong, "Effect of atomic-level stresses on local dynamic and mechanical properties in CuxZr100−x metallic glasses: a molecular dynamics study," *Intermetallics*, vol. 58, pp. 50–55, 2015.

[31] M. Imran, F. Hussain, M. Rashid, Y. Cai, and S. A. Ahmad, "Mechanical behavior of Cu—Zr bulk metallic glasses (BMGs): a molecular dynamics approach," *Chinese Physics B*, vol. 22, no. 9, Article ID 096101, 2013.

[32] C. D. Wu, "Molecular dynamics simulation of nanotribology properties of CuZr metallic glasses," *Applied Physics A*, vol. 122, no. 4, p. 486, 2016.

[33] S. Plimpton, "Fast parallel algorithms for short-range molecular dynamics," *Journal of Computational Physics*, vol. 117, pp. 1–19, 1995.

[34] C. Braga and K. P. Travis, "A configurational temperature Nosé-Hoover thermostat," *The Journal of Chemical Physics*, vol. 123, no. 13, Article ID 134101, 2005.

[35] A. Stukowski, "Visualization and analysis of atomistic simulation data with OVITO–the Open Visualization Tool," *Modelling and Simulation in Materials Science and Engineering*, vol. 18, no. 1, Article ID 015012, 2009.

[36] K. Song, S. Pauly, Y. Zhang et al., "Significant tensile ductility induced by cold rolling in Cu47. 5Zr47. 5Al5 bulk metallic glass," *Intermetallics*, vol. 19, no. 10, pp. 1394–1398, 2011.

[37] M. Stolpe, J. J. Kruzic, and R. Busch, "Evolution of shear bands, free volume and hardness during cold rolling of a Zr-based bulk metallic glass," *Acta Materialia*, vol. 64, pp. 231–240, 2014.

[38] R. Martinez, G. Kumar, and J. Schroers, "Hot rolling of bulk metallic glass in its supercooled liquid region," *Scripta Materialia*, vol. 59, no. 2, pp. 187–190, 2008.

[39] S. Feng, L. Qi, L. Wang et al., "Atomic structure of shear bands in Cu64Zr36 metallic glasses studied by molecular dynamics simulations," *Acta Materialia*, vol. 95, pp. 236–243, 2015.

[40] H. Yan, Y. Hu, Z. Yan, X. Zheng, and Y. Li, "Microstructure evolution of Zr50Cu18Ni17Al10Ti5 bulk metallic glass during cold-rolling," *Journal of Materials Science & Technology*, vol. 28, no. 8, pp. 756–760, 2012.

[41] W. Cui, J. Pan, D. J. Blackwood, and Y. Li, "Voronoi volume recovery during plastic deformation in deep-notched metallic glasses," *Journal of Alloys and Compounds*, vol. 776, pp. 460–468, 2019.

[42] S. Trady, M. Mazroui, A. Hasnaoui, and K. Saadouni, "Molecular dynamics study of atomic-level structure in

monatomic metallic glass," *Journal of Non-crystalline Solids*, vol. 443, pp. 136–142, 2016.

[43] N. Amigo and F. Valencia, "Mechanical and structural assessment of CuZr metallic glasses rejuvenated by thermal-pressure treatments," *Computational Materials Science*, vol. 198, Article ID 110681, 2021.

[44] N. Amigo, F. Urbina, and F. Valencia, "Shear transformation zones structure characterization in Cu50Zr50 metallic glasses under tensile test," *Computational Materials Science*, vol. 184, Article ID 109941, 2020.